Antiviral Research 89 (2011) 246–256

Contents lists available at ScienceDirect

Antiviral Research

journal homepage: www.elsevier.com/locate/antiviral

High-content screening to distinguish between attachment and post-attachment steps of human cytomegalovirus entry into fibroblasts and epithelial cells

Yvonne Ibig-Rehm[a,1], Marjo Götte[a,1], Daniela Gabriel[a], David Woodhall[b], Ashley Shea[b], Nathan E. Brown[b], Teresa Compton[b], Adam L. Feire[b,*]

[a] Lead Finding Platform, Novartis Institutes for Biomedical Research, Forum 1, Novartis Campus, CH-4056 Basle, Switzerland
[b] Infectious Diseases, Novartis Institutes for Biomedical Research, 500 Technology Square, Cambridge, MA 02139, USA

ARTICLE INFO

Article history:
Received 6 November 2010
Received in revised form 13 January 2011
Accepted 21 January 2011

Keywords:
HCMV
Cytomegalovirus
High-content screening
Imaging
Virus entry

ABSTRACT

Human cytomegalovirus (HCMV) enters cells through a complex pathway involving the interaction of multiple viral glycoproteins and cellular receptors. While HCMV clinical isolates enter a wide range of cell types, entry has historically been studied using a laboratory strain of virus that can only infect fibroblasts. Herein, we have constructed a HCMV reporter strain that contains GFP fused to the abundant tegument protein pp65 to allow for the direct visualization of virus attachment and entry. Furthermore, the UL131 gene of this strain was restored to clinical isolate sequence to expand our studies of entry into physiologically relevant epithelial cell types. Using the HCMV-GFP reporter virus, we developed an image-based assay and screened a library containing 65,000 compounds for the inhibition of virus entry into fibroblasts. In addition to assessing the effect on virus entry, automated image analysis provided information on compound toxicity and whether the compounds acted as attachment or post-attachment inhibitors. To identify therapeutically viable inhibitors capable of blocking entry in multiple cell types, the inhibitors were screened further for their ability to inhibit virus entry into epithelial cells. Compounds were identified that were able to inhibit virus entry into both cell types at either attachment or post-attachment steps.

1. Introduction

Human cytomegalovirus (HCMV) is the prototypical member of the beta-*Herpesviridae*. As such, infection is life-long and usually asymptomatic. However, HCMV infection is a significant cause of morbidity and mortality in immunocompromised patients, including chemically immunosuppressed transplant patients and immune naive pregnant women (Griffiths et al., 2000; Jacobson, 1998; Ljungman, 1996; Whitley, 2004). Currently there is no vaccine available for the prevention of HCMV disease and the high degree of toxicity associated with the current nucleoside-based antiviral therapies precludes their use in pregnant women and limits their use in the transplant setting (Griffiths et al., 2000). Thus, additional antiviral therapies with reduced toxicity and novel mechanisms of action are needed to effectively combat CMV disease in both these settings.

HCMV can cause disease in a wide range of organ systems and tissue types. This broad tissue tropism is made possible by the ability of clinical isolates of the virus to enter and initiate replication in a wide range of diverse cell types, including epithelial cells, endothelial cells, fibroblasts, and monocyte-derived macrophages (Cinque et al., 1997; Dankner et al., 1990; Ibanez et al., 1991; Nowlin et al., 1991; Sinzger and Jahn, 1996; Sinzger et al., 2000; Sweet, 1999; van Den Pol et al., 1999). Until recently, most studies characterizing the entry pathway of HCMV have focused on fibroblast-adapted laboratory strains of the virus such as AD169, which are unable to infect epithelial and endothelial cells. The use of fibroblast adapted laboratory strains was primarily due to the relatively fast growth and high titers obtained during *in vitro* culture. However, it has become increasingly clear that the entry pathway of fibroblasts and the other physiologically relevant cell types are not identical (Compton, 1995; Compton et al., 1992; Ryckman et al., 2008; Sinzger, 2008).

To enter fibroblasts, HCMV first requires a tethering step that is mediated by viral glycoprotein B (gB) and glycoproteins M and N (gM/gN) (Boyle and Compton, 1998; Compton et al., 1993; Kari and Gehrz, 1992). This interaction is followed by a more stable interaction between gB and one of multiple proposed growth factor receptors of the host cell (Boyle and Compton, 1998; Soroceanu et al., 2008; Wang et al., 2003). Further post-attachment inter-

* Corresponding author at: Novartis Institutes for Biomedical Research, Infectious Diseases, 500 Technology Square, Cambridge, MA 02139, USA. Tel.: +1 617 871 7905; fax: +1 617 871 5867.
E-mail address: adam.feire@novartis.com (A.L. Feire).
[1] These authors contributed equally to this work.

0166-3542/$ – see front matter © 2011 Elsevier B.V. All rights reserved.
doi:10.1016/j.antiviral.2011.01.007

actions between gB and gH/gL with Beta 1 and Beta 3 integrins, respectively, ultimately drive virus-cell fusion at the plasma membrane at neutral pH (Feire et al., 2004, 2010; Wang et al., 2005).

Like fibroblast entry, HCMV entry into epithelial and endothelial cells requires a gB interaction with Beta 1 integrin (Feire et al., 2010). However, recently it has been demonstrated that infection of epithelial and endothelial cells requires an intact UL131 gene locus, which enables the virus to express an additional pentameric gH-containing complex (Gerna et al., 2005; Hahn et al., 2004; Wang and Shenk, 2005a,b). This pentameric complex contains glycoproteins H and L along with the gene products from UL128, UL130, and UL131a and has been shown to be incorporated into virions and be important during virus entry into epithelial and endothelial cell, but not fibroblasts (Wang and Shenk, 2005b).

Thus, a useful HCMV antiviral therapeutic working at the entry step of the lifecycle would need to inhibit both the fibroblast and epithelial cell entry pathways. Towards this end we have constructed an AD169 reporter virus that contains UL83 fused to GFP. The UL83 gene encodes for pp65, which is highly abundant in the virion tegument accounting for 90% of the tegument mass and 45% of the virion mass (Jahn et al., 1987a,b; Ruger et al., 1987; Roby and Gibson, 1986; Somogyi et al., 1990; Varnum et al., 2004). As part of the incoming virion, pp65 is targeted to the nucleus immediately after infection (Schmolke et al., 1995). The AD169-pp65GFP virus allows for tracking of virus binding, fusion, and nucleocapsid trafficking to the nucleus in fibroblasts, but not other cell types. To restore the ability of AD169-pp65GFP to infect epithelial and endothelial cells we used homologous recombination to repair the UL131 gene locus back to clinical isolate VR1814 sequence. The resultant AD169-pp65GFPrUL131 reporter virus expresses a fully functional pentameric gH complex and subsequently has the broad cellular tropism found in HCMV clinical isolates.

To identify low molecular weight compounds that inhibit the pentameric gH complex-mediated entry of HCMV as well as the entry into fibroblasts we developed a high-content imaging-based high-throughput assay that uses GFP-tagged pp65 to differentiate between attachment and post-attachment steps of both fibroblast and epithelial cell types.

2. Materials and methods

2.1. Cell culture

Primary normal human dermal fibroblasts (NHDF), human foreskin fibroblasts (HFF) and human epithelial cells derived from pigmented retina (ARPE-19) were supplied by Lonza. NHDF and HFF cells were propagated in Dulbecco's modified Eagle's medium (DMEM) with high glucose (Gibco) supplemented with 10% fetal calf serum (FCS, Gibco) and 1% L-glutamine (Gibco). ARPE-19 cells were propagated in DMEM:F12 (Gibco) medium supplemented with 10% FCS. FCS was omitted when the cells were infected with CMV.

2.2. Construction of AD169-pp65GFP

In order to clone a virus encoding for a pp65 (UL83 gene product) tagged with eGFP, an *eGFP* cassette was cloned immediately downstream of the UL83 gene in strain AD169 of HCMV, with the deletion of the *UL83* stop codon. The cloning strategy was based upon the 'recombineering' protocol previously described (Warming et al., 2005) and the AD169 strain of HCMV cloned as a BAC (pAD/Cre) (Yu et al., 2002). pAD/Cre contains the full-length AD169 with the BAC cassette flanked by LoxP sites inserted immediately after the *US28* ORF, without the deletion of any viral sequences. The BAC vector contains the Cre recombinase-encoding gene, disrupted by an intron, under the control of the simian virus 40 promoter. When purified pAD/Cre is electroporated into primary human foreskin fibroblasts (HFFs), Cre is expressed and mediates site-specific recombination between the two LoxP sites, excising the BAC cassette and yielding a wild-type genome with the exception of a 34 bp insert remaining of the LoxP site.

Firstly, pAD/Cre was cloned into the SW102 strain of *E. coli*. Cloning mutant BACs in SW102 is a two-step procedure. First, a *galK* cassette containing 50 bp homology arms to *UL83* (without the stop codon) and the region immediately downstream of *UL83* was generated by PCR and cloned by homologous recombination into pAD/Cre in the precise desired location of the *eGFP* insert. Recombinants were selected by growth on medium in which galactose was the only carbon source, enriching for bacteria which contained the *galK* insert. In the second step, the *galK* gene was substituted with the *eGFP* cassette with homology arms to *UL83* and the region immediately downstream of *UL83* and recombinants were selected on growth medium containing 2-deoxy-galactose (DOG), and glycerol, as carbon sources. Galactokinase catalyses the phosphorylation of the galactose analog, which produced a toxic by-product (2-deoxy-galactose-1-phosphate) that enriched for bacteria that lost the *galK* cassette in place of *eGFP*.

2.2.1. Preparation of BAC DNA

BAC DNA was prepared using a "Spin Doctor Super Clean BAC Prep Kit" from Gerard Biotech (Cat# SL120L). BAC DNA was resuspended in 200 μl of ddH_2O and prepared within a week of being used for electroporation of bacterial or mammalian cells.

2.2.2. Homologous recombination

To amplify the *galK* cassette with homology arms to the 5′ end of *UL83*, the following primers were used: UL83-galK-fwd ACGCCTTGCCCGGGCCATGCATCGCCTCGACGCCCAAAAAGCACCGAGGTCCTGTTGACAATTAATCATCGGCA and UL83-galK-rvrs AGTGGACGTGGGTTTTTATAGAGTCGTCCTAAGCGCGTGCGGCGGGTGGCTCAGCACTGTCCTGCTCCTT, underlined regions denote primer sequence for amplification of *galK*. Primers were diluted to 25 pmol/μl. To amplify the *eGFP* cassette with homology arms to the 5′ end of UL83, the following primers were used: AGTGGACGTGGGTTTTTATAGAGTCGTCCTAAGCGCGTCCGGCGGGTGGCTTACTTGTACAGCTCGTCCAT and ACGCCTTGCCCGGGCCATGCATCGCCTCGACGCCCAAAAAGCACCGAGGTATGGTGAGCAAGGGCGAGGAG. Underlined sequences denote homology to *eGFP*.

2.2.3. Screening for correctly recombined clones

In order to screen for correctly recombined BACs containing the *eGFP* cassette, a colony PCR-based screen was developed. Colonies were picked from the plates into 1 ml of LB broth containing chloramphenicol (12 μg/ml) in a 96-well plate and grown overnight with shaking at 32 °C. The following day, 2.0 μl of this culture was used to provide template in the following colony PCR reaction containing: 0.25 μl ExTaq DNA polymerase (Takara Biotech Cat# RR001), 50 pmol primers, 10 mM dNTP and 5.0 μl of the buffer provided by the manufacturer. The following cycler conditions were used: 94 °C for 5 min, then 30 cycles of 94 °C for 15 s, 55 °C for 30 s and 72 °C for 1 min. The primers CGCCGTTGTCCCGAAATGAT (forward) and CAGGGGATGCGCAAAGGTGAACG (reverse) were designed 500 bp either side of the *UL83* region, and were used to amplify the region such that different sized PCR products could be used to identify the correctly recombined clones. Specifically, wild-type BAC gave a 1831 bp product, the *GalK* insertion 2979 bp, and the *eGFP* insertion 2551 bp.

2.2.4. Preparation of AD169-pp65GFP virus

BAC DNA was prepared for electroporation using "Spin Doctor Super Clean BAC Prep Kit" from Gerard Biotech (Cat# SL120L).

HFF cells were fed with fresh DMEM-10 (Invitrogen) 2–4 h prior to electroporation. To prepare the cells for electroporation, they were washed with PBS before trypsinization in 0.25% trypsin (Invitrogen). Cells were pelleted by centrifugation (1600 rpm, 5 min) before resuspending in DMEM to an approximate concentration of 2.0×10^7 cells/ml.

In a 15 ml Falcon tube, 15 μl of BAC DNA suspension was combined with 1.0 μg of pCAG-pp71 plasmid and 5×10^6 HFFs in a total volume of 265 μl. The DNA-cell mixture was then transferred to a 0.4 cm cuvette and electroporated using the following conditions: 260 V and 960 μF. Cells were then seeded into a 10 cm dish and fed with DMEM 2% FBS. Fresh medium was used to feed the cells the following day and thereafter every 2 days. One week post-electroporation, cells were trypsinized and transferred to a T150 flask and fed with DMEM 2% FBS for a further two weeks, without medium change, at which point green fluorescent plaques were observed. When cytopathic effect (CPE) had spread throughout the T150 flask, the virus containing media was harvested and used as stock.

2.2.5. Virus growth curves

HFF cells were used as monolayers in determining virus growth curves by plaque assay. For multi-step growth curves, 2×10^5 HFF cells/well in a 12-well dish (Corning) were seeded a day prior to infection. The following day, cells were infected at an MOI 0.01 PFU/cell and incubated for 90 min at 37 °C. After the incubation period, the virus containing medium was replaced with fresh DMEM 2% FBS. 1 ml of medium from infected cells was harvested at 3–4-day intervals for 21 days.

The infected cell supernatants were stored at −70 °C until the end of the experiment. The samples of media were thawed, cleared of cell debris by centrifugation and the virus titer determined by plaque assay.

2.2.6. Plaque assay

1×10^5 HFF cells were seeded per well of a 6-well plate. Serial dilutions of virus were made for each of the time-points described. 500 μl of each virus dilution between 10^{-2} and 10^{-7} was added to a cell monolayer for each time-point. Each time-point was assayed in triplicate. Cells were incubated at 37 °C for 90 min with manual rocking every 20 min. A 1% agarose solution (Fisher) was prepared, autoclaved prior to use and stored in a 50 °C water bath to keep it in the liquid phase. 2XDMEM was stored in a 37 °C water bath until use. Immediately prior to addition to the cell monolayers, a 1:1 mix of agarose solution and 2XDMEM was made.

After the 90 min incubation, the virus-containing media was aspirated from the cell monolayers and cells were washed 3 times with 2 ml of PBS. 1.5 ml of the DMEM/agarose solution was added to each monolayer and allowed to solidify at room temperature (RT) for 10 min. Cells were incubated overnight. The following day, 2 ml of DMEM 2% FBS was added to each well. Cells were incubated for 2–3 weeks, with medium changes every 2–3 days, until large plaques had developed.

To fix and stain plaques, medium was aspirated and 2 ml of a 4% paraformaldehyde solution in PBS was added to each well, on top of the agarose plug. Plates were incubated at RT for 30 min, after which the paraformaldehyde was discarded and the agarose plugs carefully removed with a spatula. Wells were stained with 0.5 ml of methylene blue for 15 s before thorough rinsing (4 times) with dH_2O.

2.3. Construction of AD169-pp65GFP-UL131restored

2.3.1. Generation of UL131 and UL132 gene products

A DNA fragment containing the functional UL131 and UL132 genes was generated by amplifying the complete UL131 reading frame from the VR1814 strain of CMV. The fragment was 1430 bp and was amplified using the following primers: VR-UL132 (5′- *ATG CCG GCC CCG CGG G* -3′) and VR-UL131 (5′- *CCC GTG ACG CAG GCT AGT* -3′). This fragment contained the complete VR1814 UL132 and UL131 genes with a homology region that extends outside the UL131 reading frame 30 bp downstream. Amplification was performed by PCR using primers at a concentration of 25 μM and mixing them with 2.5 units of Taq (Invitrogen, CN 18038-042), 1 mM dNTP, 150 ng of VR1814 DNA. This solution was incubated at 94 °C for 20 s, then 30 cycles of; 94 °C for 20 s, 60 °C for 20 s, 72 °C for 2.5 min. The fragment was purified from a 1.2% agarose TAE gel using the Zymoclean™ Gel DNA Recovery Kit (Zymo Research, CN D4002).

2.3.2. Recombination

NHDF cells were infected with wtAD169-GFP in T150 flasks at a MOI of 1. Three days post-infection the infected cells were transfected with 12 μg of each fragment using Lipofectamine 2000 (Invitrogen, CN 11668-027) as directed by the manufacturer. Flasks were incubated at 37 °C until 90% CPE was observed. Recombined AD169 viruses harvested from NHDF cells were used to infect ARPE-19 cells. At 29 days post infection both flasks showed 95% CPE and were harvested as described previously (1). Harvested viruses were passaged once more in ARPE-19 cells and harvested. The UL132–UL131 region of each virus was sequenced to verify the correct insertion of the VR1814 UL131–UL132 gene fragment.

2.3.3. Virus infectivity assay

12,000 cells per well were plated in 96-well plates (Costar) and incubated overnight at 37 °C in 5% CO_2. Cells were washed three times in serum free media before virus was added at the indicated inoculums at 37 °C in 5% CO_2. 3 h post-infection (p.i.) the virus was replaced with complete media and the cells returned to 37 °C in 5% CO_2. 24 h p.i. the cells were fixed in 4% paraformaldehdye (PFA) for 20 min at room-temperature. The cells were washed three times in 1× PBS before permeabilization in 1× PBS containing 0.1% Triton-X for 10 min at room-temperature. Cells were then stained with a mouse monoclonal anti-IE antibody (1:2000) for 1 h followed with an anti-mouse Alexa Fluor 594 conjugated secondary antibody (1:3000) for 1 h. Cells were counterstained with 4′,6′-diamidino-2-phenylindole dihydrochloride (DAPI) (1:5000). The number of cells and the percent of IE positive cells were counted using Cellomics Arrayscan.

2.4. Control compounds and compound preparation

Heparin (Sigma), dissolved in water, and a bis-(aryl)thiourea inhibitor (Novartis compound archive, Bloom et al., 2003, see Fig. 3) dissolved in DMSO, were used as control compounds. The bis-(aryl)thiourea inhibitor will be referred in the text as thiourea compound.

Compounds to be screened were dissolved in 90% DMSO. In primary screening, final compound concentration was 10 μM and final concentration of DMSO was 0.5%. In validation, the compounds were analyzed in quadruplicate with eight concentrations. The highest compound concentration was 20 μM, and the lowest concentration was 6 nM. The final concentration of DMSO was 1%. For calculation of % inhibition, the DMSO controls in column 23 were used as a negative and 100 nM thiourea compound in column 24 was used as a positive control.

2.5. Viral entry assay

Cells were seeded at a density of 4000 (NHDF) or 7000 (ARPE-19) cells per well in a volume of 30 μl in 384-well assay plates (Corning) using serum-free culture medium the day before the

experiment. Next day 5 μl of compound were added using the CyBi-Well pipettor (CyBio, Jena, Germany). One hour later the cells were infected with 10 μl CMV-AD169-pp65-GFP for NHDF cells or CMV-AD169-pp65rUL131-GFP for ARPE-19 cells, respectively. Six (NHDF) or 8 h (ARPE-19) after virus infection the cells were fixed and the nuclei stained by adding paraformaldehyde (PFA, Electron Microscopy Sciences) and DRAQ5 (Alexis) to final concentrations of 4% and 0.125 μM, respectively. The cells were incubated for 15 min in the dark, washed twice with 50 μl phosphate-buffered saline (PBS), and were then kept at 4 °C in the dark until imaging.

2.6. Phalloidin staining

Cells were fixed with 4% PFA, washed with PBS and then permeabilized and blocked with 0.1% Triton X-100, 10% FCS in PBS for 30 min at RT. The cells were incubated with 3 U of Alexa Fluor 647-conjugated phalloidin (Invitrogen) and 1 μg/ml Hoechst 33342 (Invitrogen) for 30 min at RT in the dark. The cells were washed twice with PBS and kept in PBS in the dark until imaging.

2.7. Image acquisition and analysis

Images were acquired with IN Cell Analyzer 3000 (GE Healthcare) automated cell imager. Flat field correction was done using a plate with various mixtures of Oregon Green (Molecular Probes), Cy5 calibration reagent (GE Biosciences) and Alexa Fluor 350 carboxylic acid (Molecular Probes). Images for DRAQ5 and for GFP were taken on two different channels with two CCD cameras simultaneously. DRAQ5 was excited with the 647 nm krypton laser, and 695/BP55 emission filter was used to collect the emitted light. GFP was exited with the 488 nm line of the argon laser, and 535/BP45 emission filter was used to collect the emitted light. Exposure time for both channels was 1.7 ms.

Image analysis was performed using various modules of the IN Cell Analyzer 3000 software. The percentage of infected cells (%Fpass) was analyzed using the object intensity module OBI1. An intensity threshold was set on the green signal channel in a defined nuclear region. The cells passing the set threshold were regarded as infected by the virus.

The ratio of nuclear and cytoplasmic intensity of GFP (Nuc/Cyt) was analyzed using the nuclear trafficking module TRF2, which measures the fluorescence intensity of GFP in the nuclear region and in a ring around the nucleus (cytoplasm), and calculates the ratio of these intensities.

The variable grain size module VGS0 was used to differentiate two types of inhibition of virus entry. The nuclear area was dilated by 30 pixels to define the area where the software identified granules. The granules had to fit to a boundary box of 7 × 7 pixels (1 pixel equals 0.6 μm) and the intensity had to be between 243 and 1638 units in order to be calculated as granules. This gating excluded viral aggregates that were larger and had an average intensity of 3200–3500. The readouts reported by the module include number, area and fluorescence intensity of the granules.

The number of cells was reported by all modules and was used as an indication of compound toxicity.

2.8. Data analysis and curve fitting

Percent activity of the compounds was calculated from the formula: % inhibition = 100 × (value of sample − value DMSO control)/(value of 100 nM thiourea control − value of DMSO control). The dose-response curves (DRC) data were fitted with a four parameter logistic function using a Novartis internal screening analysis software. Z' was calculated as described (Zhang et al., 1999).

3. Results

3.1. Generation of HCMV pp65-GFP reporter viruses capable of infecting multiple cell types

To track the entry and post entry steps of HCMV infection of human fibroblasts a GFP reporter virus was constructed by fusing GFP to the C-terminus of UL83 (pp65). The UL83 gene product pp65 is the most abundant protein packaged within HCMV virions (Varnum et al., 2004). Thus, at 2 h post infection the GFP-tagged virions can be directly visualized binding to cells and subsequent to fusion and nucleocapsid trafficking accumulating in the nucleus (Fig. 1a). Once a cell is infected, *de novo* pp65-GFP is expressed with early kinetics with a strong nuclear GFP signal observed 24 h p.i. (Fig. 1a). At later timepoints, coinciding with the production of structural components and packaging of daughter virions, pp65-GFP is found both in the nucleus and in the surrounding ER and Golgi (Fig. 1a).

The creation of a fusion protein and resulting addition of genetic material to a virus can lead to deleterious growth kinetics from either the altered function of the wild type protein or through inefficient packaging of the larger DNA genome (Menard et al., 2003). To test the growth kinetics of the AD169 pp65-GFP a multistep growth curve was performed. Over the course of a 20 day infection, approximately equivalent growth kinetics and peak titers were observed for both wild type and pp65-GFP HCMV (Fig. 1b). These data confirm that the construction of the AD169 pp65-GFP reporter virus did not result in significant fitness cost to the virus.

The incorporation of UL131a, UL130, and UL128 gene products into HCMV virions has previously been shown to be required for HCMV entry of epithelial, endothelial and dendritic cells (Gerna et al., 2005; Hahn et al., 2004; Wang and Shenk, 2005a,b). To track entry and post entry steps of HCMV infection in cell types other than human fibroblasts, the AD169-pp65GFP virus was modified by homologous recombination to restore the UL131 gene locus found in the clinical isolate VR1814. In brief, NHDF cells were infected with AD169-pp65GFP and allowed to begin replication. Cells were then transfected with the appropriate UL131 DNA fragment containing sufficient homology arms on both 3′ and 5′ ends of this gene locus. Virus was harvested 7 days post infection and used to infect ARPE-19 cells, which can be infected only with a virus containing an intact UL131 locus. The intact UL131 gene locus was then sequence confirmed (data not shown). To further confirm that the UL131 gene was properly recombined into AD169-pp65GFP and that the clinical isolate tropism had been restored, a comparison of the cellular tropism of the two reporter viruses was performed. At 3 days post infection, HCMV CPE and pp65-GFP was clearly observed in the epithelial cell infection of AD169rUL131 (Fig. 2b), but not AD169-pp65GFP (Fig. 2a). To quantitatively measure the restoration of cellular tropism of AD169rUL131, we next compared the percent of infected epithelial cells (ARPE-19), endothelial cells (HUVEC), or fibroblasts (NHDF) in response to increasing amounts of either virus. Increasing AD169-pp65GFP resulted in a MOI-dependent increase in the number of fibroblast infected cells; while relatively little infection was observed in epithelial or endothelial cells (Fig. 2c). In contrast, the AD169rUL131 reporter virus infected all cell types tested in a MOI-dependent manner (Fig. 2d). These data confirm the function restoration of tropism of the AD169rUL131 reporter virus.

3.2. Effect of heparin and the thiourea compound on virus entry in NHDF and ARPE cells

Heparin is known to bind to the gM/gN heterodimer and gB glycoprotein complexes of the HCMV envelope, thereby inhibiting the tethering of the virus on the surface of host cells (Shukla et al.,

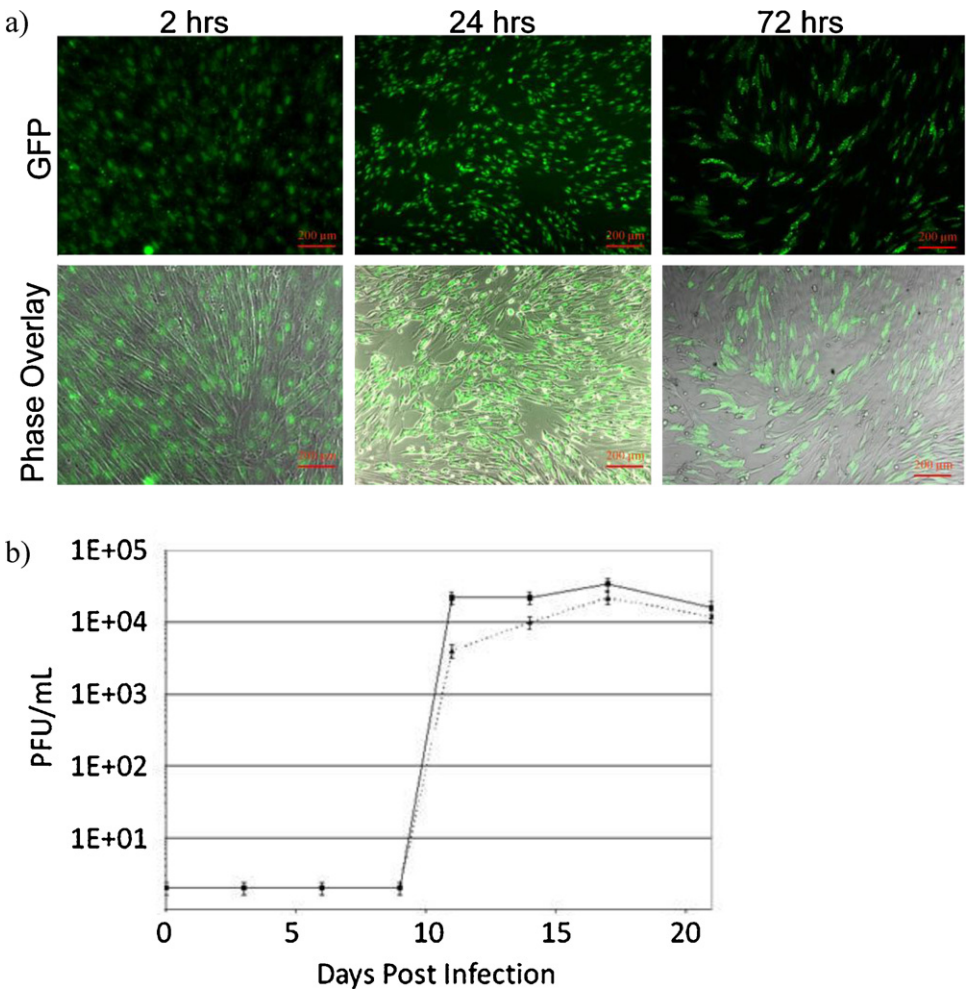

Fig. 1. Validation of AD169-pp65GFP reporter virus construction. (A) Normal human dermal fibroblasts were infected at an MOI = 3 of the AD169-pp65GFP reporter virus and imaged at the indicated times. (B) Multi-step growth curves comparing the fitness of wild type AD169 (filled line) with AD169-pp65GFP (dotted line). NHDF cells were infected with wild type AD169 or with AD169-pp65GFP at a low MOI (=0.01). Samples were harvested twice per week for three weeks. Titers at each timepoint were determined by plaque assay.

1999). A thiourea compound has been reported to inhibit virus internalization in fibroblasts downstream of the virus tethering step (Bloom et al., 2003; Jones et al., 2004). The effect of heparin and the thiourea compound on HCMV entry to fibroblasts and epithelial cells was tested.

NHDF and ARPE-19 cells were treated with heparin or the thiourea compound and infected with the pp65-GFP reporter virus carrying the intact UL131 gene. Six or eight hours later, respectively, the cells were fixed and the percentage of infected cells was analyzed. Heparin decreased the percentage of infected NHDF cells with an IC_{50} value of 0.29 μg/ml, whereas the IC_{50} value for the ARPE-19 cells was 15-fold higher, 4.4 μg/ml (Fig. 3 and Table 1).

Table 1
IC_{50} values for heparin and the thiourea compound in inhibition of virus entry.

Readout	% Infected cells		Nuc/Cyt ratio	
	NHDF	ARPE-19	NHDF	ARPE-19
Compound				
Heparin	0.29	4.4	0.31	4.5
Thiourea compound	2.8	1.7	2.5	1.8

The IC_{50} values were calculated by analyzing the same set of images with two different analysis modules, object intensity for % infected cells, and nuclear trafficking for the nuc/cyt ratio. The values for heparin are in μg/ml and for the thiourea compound in nM.

The thiourea compound inhibited virus infection in both cell lines equally, the IC_{50} values being 2.8 nM and 1.7 nM, for NHDF and ARPE-19 cells, respectively. The pp65-GFP fusion protein migrates to the nucleus in infected cells. Therefore analyzing the nuclear vs. cytoplasmic ratio of the pp65-GFP intensity can be also used as a readout for effective virus infection. The nuclear vs. cytoplasmic ratio provided almost identical IC_{50} values as the analysis of percent infected cells (Table 1).

The cells treated with heparin or the thiourea compound had different phenotypes. In non-treated cells virus infection could be visualized as accumulation of the pp65-GFP in the nucleus (Fig. 4A). Cells treated with the thiourea compound had green fluorescent virus particles visible at the cell surface, indicative of a post-attachment inhibition. In contrast, cells treated with heparin had no visible virus, except for a few viral aggregates, indicative of inhibition of virus attachment. The difference in phenotype was quantified by analyzing the images with the granularity module of the IN Cell Analyzer 3000 software. In the images viral aggregates can be detected in addition to the green fluorescent virus particles (Fig. 4A). The viral aggregates could be excluded from image analysis based on their larger size and higher fluorescence intensity as described in Section 2. The analysis indicated that the area of the granules was more than two-fold in the thiourea-treated cells compared to non-treated cells, whereas heparin reduced the area of granules compared to the non-treated cells (Fig. 4C).

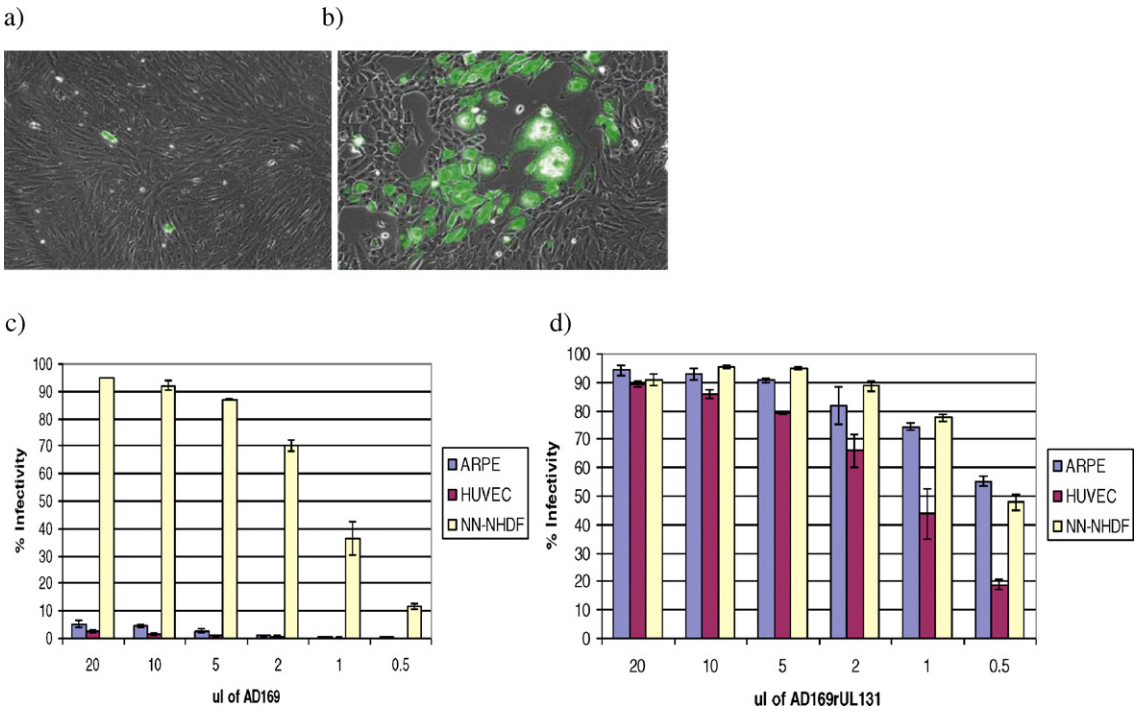

Fig. 2. Validation of AD169-rUL131 reporter virus construction. ARPE-19 cells were infected with AD169-pp65GFP (A) or AD169rUL131 (B) at a MOI = 0.5. Cells were imaged 3 days post infection. ARPE-19, HUVEC, or NHDF cells were infected with AD169-pp65GFP (C), or AD169-rUL131 (D) at the indicated volumes of virus stock. Cells were assayed for percent infectivity by quantifying the percent immediate early protein positive nuclei per total DAPI stained nuclei.

However, heparin and the thiourea compound inhibited equally infection of the cells (Fig. 4B). Thus, the granularity module could be used distinguish between two modes of inhibition of virus entry.

3.3. Primary screening

To screen for inhibitors of HCMV entry a set of 65,000 compounds was compiled. The selected compounds included a

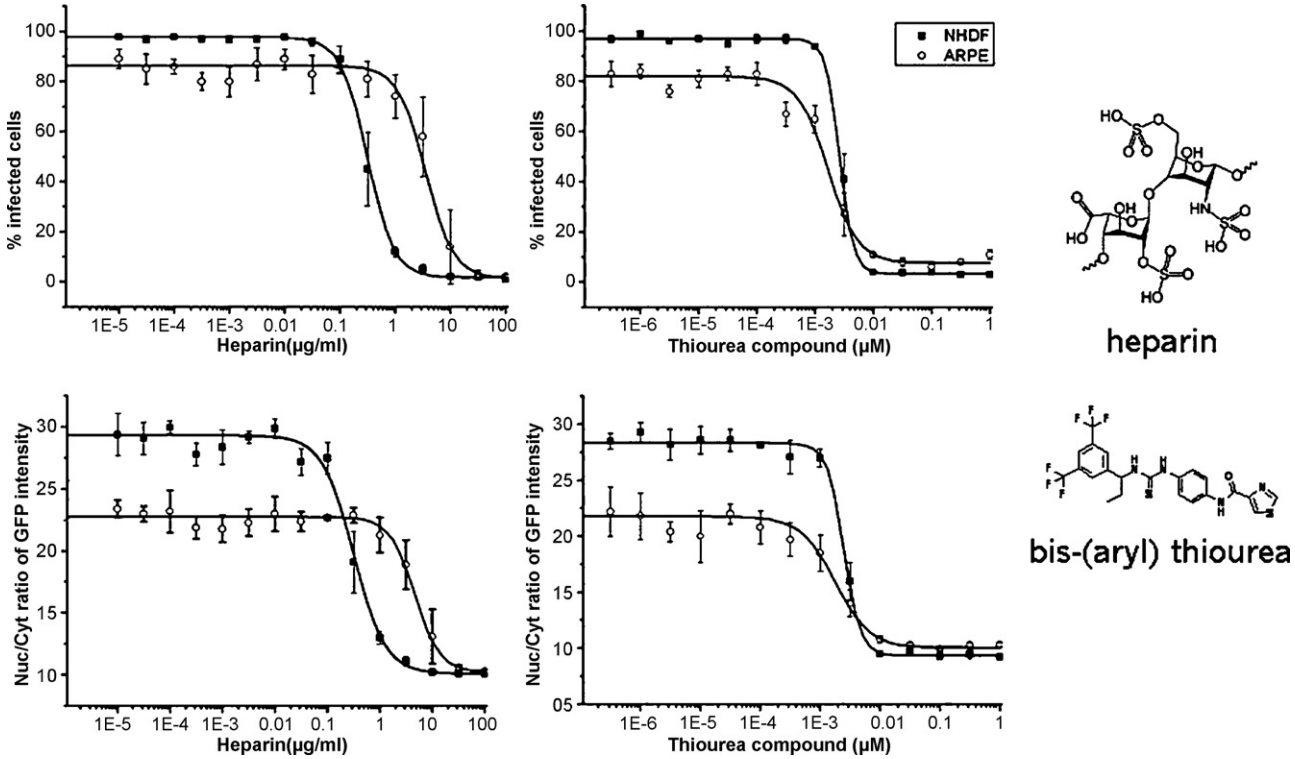

Fig. 3. Effect of heparin and the thiourea compound on virus entry in fibroblasts (NHDF) and epithelial cells (ARPE-19). Heparin or the thiourea compound was added to the cells 1 h before virus infection. The cells were fixed 6 h (NHDF) or 8 h (ARPE-19) after virus infection. Images were acquired with IN Cell Analyzer 3000 and analyzed with the object intensity module to obtain the % infected cells and with the nuclear trafficking module to obtain the nucleus/cytoplasm ratio of GFP intensity ($n = 4$). The structures of heparin and the thiourea compound are shown on the right.

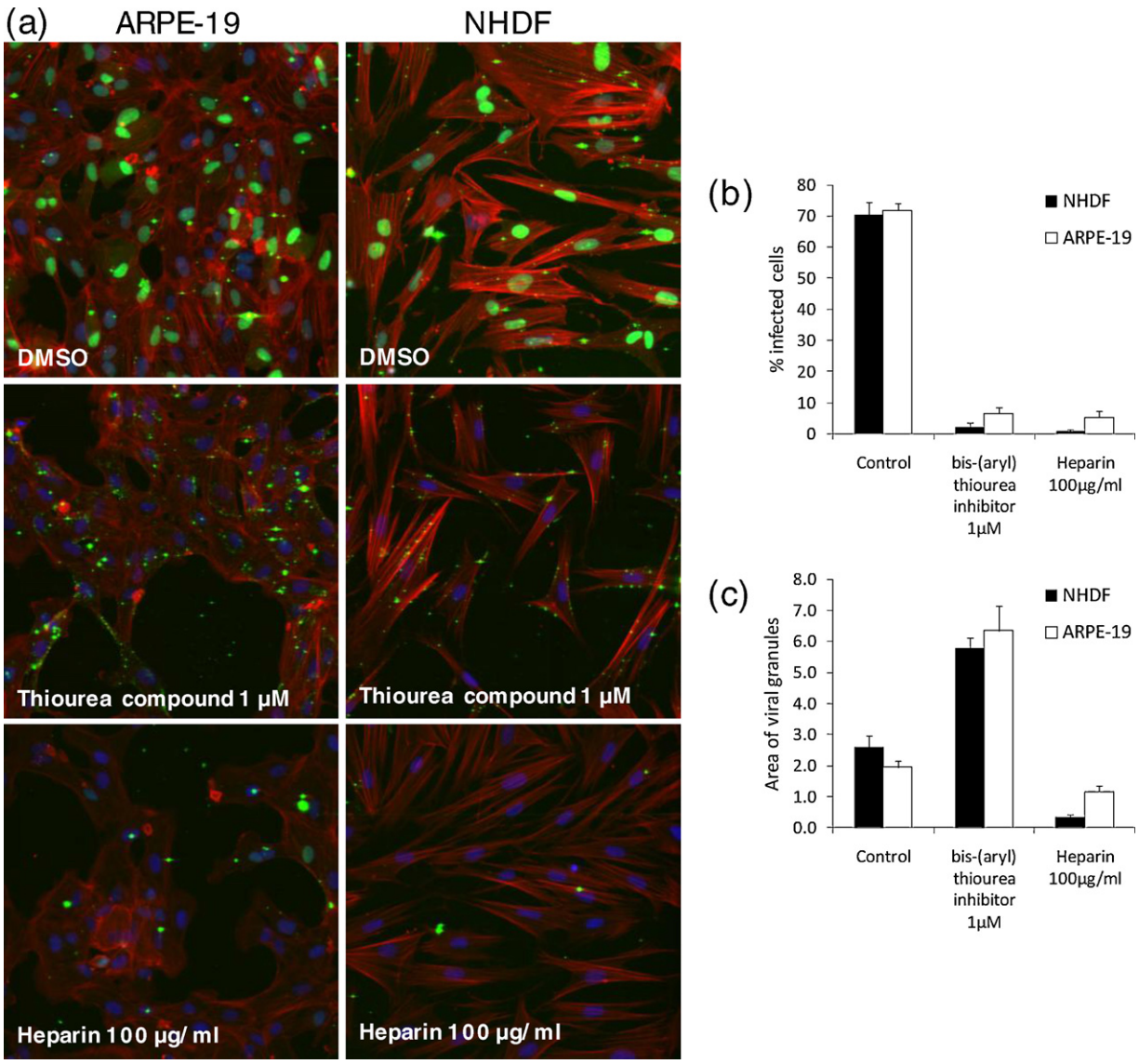

Fig. 4. Inhibition of HCMV entry is phenotypically different in heparin or thiourea compound-treated cells. (a) Images of fibroblasts (NHDF) and epithelial cells (ARPE-19) treated with DMSO, thiourea compound or heparin. Green, pp65-GFP; red, phalloidin staining to visualize actin filaments; blue, Hoechst 33342 staining to visualize nuclei. (b) Quantification of inhibition of virus entry by the object intensity module. (c) Quantification of virus particles by the variable grain size module. (For interpretation of the references to colour in this figure legend, the reader is referred to the web version of this article.)

Table 2
Compounds screened.

Compound class	No of cpds screened	Primary hits %	Validated hits %	% Toxic hits	% Hits with granular appearance
Natural products	11,616	6.5	2.7	29	7
Climax[a]	1590	3.7	1.3	39	17
GPCR	8664	1.7	0.6	44	35
Wnt pathway	2831	0.5	0.04	0	0
Known drugs	1834	2.8	1.1	25	19
Peptidomimetics	2886	0.2	0	0	0
Kinase inhibitors	7763	2.2	0.6	46	39
Ion channel	5073	1.5	0.4	70	15
Diversity set[b]	6688	0.8[d]	0.04[d]	1[d]	100[d]
Additional compounds[c]	15,823				
Total	64,768	2.2	0.7	34	16

[a] Lead compounds that were developed far, but not to final drugs.
[b] Diverse compounds selected as described (Crisman et al., 2007).
[c] Whole plates were selected for the screen. Some plates contained additional compounds not belonging to the above classes.
[d] The percentage was not calculated separately for the diversity compounds and additional compounds.

Table 3
Mean and standard deviation for controls and samples and selection of hits.

A	Thiourea control		DMSO control		Samples	
	mean	sd	mean	sd	mean	sd
% Infected cells	−100.0	2.5	−0.2	6.3	−1.0	11.9
Nuc/Cyt ratio	−99.9	2.2	0.0	10.7	−0.2	16.3

B	2 SD			3 SD			>35% Inhibition
	Number of hits	% Inhibition threshold	Hit rate %	Number of hits	% Inhibition threshold	Hit rate %	Number of hits
% Infected cells	1546	25%	2.39	728	37%	1.12	871
Nuc/Cyt ratio	1486	33%	2.29	785	48%	1.21	1321
Hits with both readouts	849		1.31	519		0.80	686
Total hits	2183		3.37	994		1.53	1506

B, the absolute number of hits, the corresponding hit rate and % inhibition of infection is shown for thresholds average + 2 SDs and average + 3 SDs of all samples.

collection of natural products, GPCR inhibitors, kinase inhibitors, peptidomimetics, known drugs and previously optimized compounds to various cellular targets (Table 2). Primary screening was performed using the AD169-pp65GFP infection of NHDF cells as described in Section 2.5. The thiourea compound was used as a positive control at a concentration of 100 nM, and 0.5% DMSO was used as a neutral control. The averages and standard deviations for both controls and all samples are shown in Table 3A. Hits were selected based on two readouts: percent infected cells and the nuclear vs. cytoplasmic ratio of GFP intensity. Absolute number of hits and hit rates were evaluated both for thresholds average plus 2 SDs and average plus 3 SDs of all samples (Table 3B). However, using standard deviations as thresholds would have lead to different inhibition levels of infection in the two readouts compared to the DMSO control. Thus, we chose to use a threshold of 35% or more inhibition compared to the DMSO control for both readouts (Table 3B). A compound was selected as a hit if it passed the 35% threshold on either readout. The total number of hits selected was 1506, 686 of them passed the 35% criterion with both readouts. Natural products had the highest hit rate, followed by compounds from the Climax box. The peptidomimetics had the lowest hit rate (Table 2). The assay performance was excellent for both readouts with an average Z' of 0.75 for % infected cells and an average Z' of 0.63 for the nuclear vs. cytoplasmic ratio of GFP intensity. The Z' values were calculated from the positive and neutral controls in columns 23 and 24 of the plates, respectively.

3.4. Validation of the hits

Toxic compounds resulting in very low cell number and highly fluorescent compounds, disturbing image analysis, were removed from the hit list. In the end 1364 hits were analyzed in the above imaging assay with eight concentrations and quadruplicate samples to obtain IC_{50} values. From the primary hits 476 had IC_{50} values $\leq$20 μM, whereby 35% of the hits could be validated. As with the primary hits, the natural products formed the largest group of validated hits as well (Table 2). Analysis of the images with the granularity module indicated that 78 compounds (16% of the validated hits) induced a similar phenotype as the thiourea compound, i.e., GFP-positive granules were visible at the cell surface. Thus, these compounds allowed for binding of the virus to the cell surface, but prevented later steps of virus entry. Most of the compounds with this mode of action belonged to kinase or GPCR inhibitors. All hits from the diversity set and additional compounds allowed virus tethering but prevented further steps. However, there were only 10 hits from these subclasses of compounds.

Information about compound toxicity is easily available in cellular imaging assays. Toxicity is manifested as reduced cell number, often associated with condensed nuclei having increased fluorescence intensity. From 476 validated compounds, 160 revealed cytotoxic effects with 60 compounds having IC_{50} values $\leq$10 μM, and 100 compounds having activities between 10 μM and 20 μM in the readout cell number. However, the cells were in medium lacking serum, which can sensitize them for otherwise weakly cytotoxic or even non-toxic compounds.

3.5. Effect of the validated hits in HCMV entry in epithelial cells

The effect of the validated hits on infection of the epithelial cells by HCMV was studied using the virus strain with restored UL131 gene. From 462 compounds analyzed, 349 inhibited HCMV entry into ARPE-19 cells with IC_{50} values $\leq$20 μM. Analysis of the images with the granularity module indicated that 151 compounds allowed tethering of the virus to the cell surface but prevented further internalization; 311 compounds induced a similar phenotype as heparin suggesting that they prevented attachment of the virus to the cell surface. Sixty compounds reduced the cell number.

3.6. Comparison of the hits in NHDF and ARPE-19 cells

Even though the entry mode of HCMV is different in epithelial cells and fibroblasts, 76% of the compounds were active in both cell types. However, many of the hits had differing IC_{50} values in the two cell lines with a Spearman rank correlation coefficient of 0.5 (Fig. 5). Using Bland–Altman analysis we studied whether one cell line is systematically more sensitive than the other (Bland and Altman, 1999). The average difference of the logarithm of the IC_{50} values scattered around the origin in the y-axis, which suggests that there is no shift in sensitivity towards either of the cell lines.

Comparison of the compounds' mode of action in both cell lines showed a correlation of the phenotypic appearance. 64% inhibited virus entry phenotypically similar to heparin, meaning no attachment of the virus, and 13% similar to the thiourea control compound in both cell types (Fig. 6a). A similar distribution was identified when looking at the compound classes from the respective compound sets. Among the few possible ion channel inhibitors, none of the compounds phenotype was similar to the thiourea compound, whereas the putative GPCR inhibitors were more evenly representing both phenotypic responses. Comparing their cytotoxic response, 74% of the compounds responses correlated, 64% being non-toxic in both cell lines and 10% being cytotoxic for both cell types (Fig. 6b).

4. Discussion

With the aid of the BAC technology and Cre recombinase we constructed an AD169 HCMV strain expressing a pp65-GFP fusion protein in its tegument. The AD169 strain, which lacks the gH/gL/UL128/UL130/UL131a complex, can only infect fibroblasts.

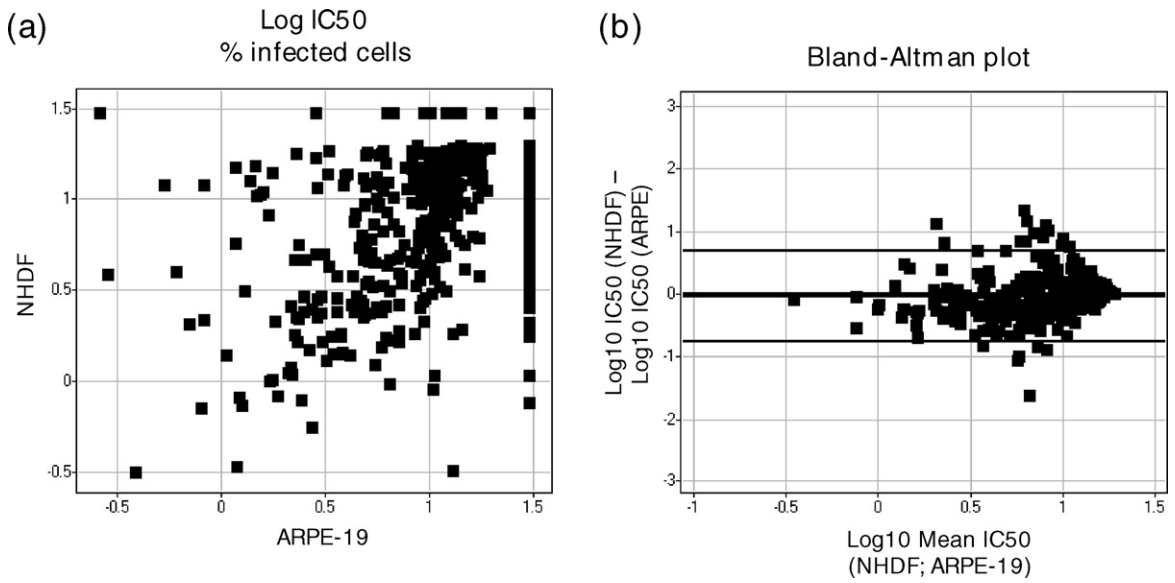

Fig. 5. Correlation of the results between epithelial cells and fibroblasts. (a) Correlation plot of the logarithm of the IC_{50} values. (b) Bland–Altman plot showing the difference of $\log_{10}$ IC_{50} values (y-axis) between NHDF and ARPE-19 cells vs. the mean of the paired $\log_{10}$ IC_{50} values (x-axis) of NHDF and ARPE-19 cells. Inactive compounds were fitted constant and are not included in the graph.

In order to also study virus entry into epithelial and other clinically relevant cell types, a second HCMV strain was constructed. The UL131 gene locus, which is required for the infection of epithelial and endothelial cells, was restored in the AD169-pp65GFP strain from a clinical isolate. The expression of the GFP fusion protein did not affect the growth kinetics of the virus, but enabled the development of a high-content screening assay for inhibitors of virus entry.

Heparin and a thiourea compound (Bloom et al., 2003) were used to develop the screening assay. Both substances inhibited virus entry into fibroblasts and epithelial cells. However, imaging revealed that the two substances had a different mode of action. Whereas heparin completely inhibited virus attachment to the cell surface, the thiourea compound allowed attachment but prevented further internalization. In the latter case the viral particles could be visualized as green dots at the cell surface. Thereby the high-content assay was not only able to identify inhibitors of virus entry, but also distinguished whether the inhibition was at the attachment or post-attachment step. The thiourea compound had the same potency in both cell types, but higher heparin concentrations were reproducibly needed to inhibit virus entry into epithelial cells than fibroblasts. One possible explanation that could account for this observation is that the primary heparin-binding glycoprotein complex, gM/gN, may be less abundant in the pentameric gH complex-containing virions that were produced in epithelial cells. Indeed, the role of heparan sulfate interactions during the entry of clinical isolates into epithelial, endothelial, and myeloid cells remains to be explored.

A set of 65,000 compounds was screened in the high-content assay using primary human fibroblasts. The hits were selected based on two readouts: percent infected cells and nuclear vs. cytoplasmic ratio of the GFP intensity. Compounds active in either

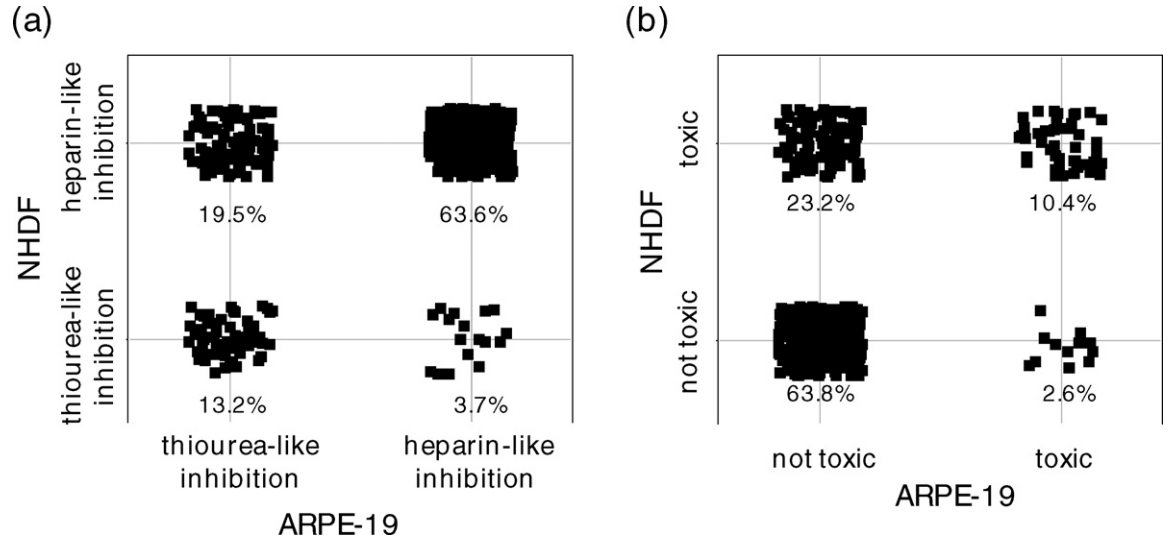

Fig. 6. Comparison of the mode of action (a) and toxicity (b) of the 349 validated compounds between fibroblasts (NHDF) and epithelial cells (ARPE-19).

readout were selected for IC_{50} determination and compound validation has proven that it was beneficial to use both readouts. By using only one or the other of the two readouts several validated hits would have been lost.

The validated hits from the fibroblast infection model were tested for their ability to inhibit entry into epithelial cells with the goal of identifying inhibitors capable of blocking both virus entry pathways. Of the validated fibroblast infection inhibitors, 76% also inhibited virus entry into epithelial cells. Moreover, from the compounds active in both cell types, 76% shared the mode of action, inhibiting the virus entry at the attachment step or post-attachment step. This indicates that there are common druggable steps in the two cell types. This observation is not surprising, since the core components of virus entry, gB, gH, gL are all essential for the entry of all cell types ([Reviewed in] Spear and Longnecker, 2003). Furthermore, recent data indicates that the gB-integrin interaction is likely a conserved feature of the entry pathway into cell types (Feire et al., 2010). Thus, it is possible that inhibitors are binding to the core glycoproteins involved in fusion or their cognate cell surface receptors.

Interestingly, a subset of compounds was able to inhibit the infection of both cell types, but through different mechanisms, e.g., compounds acting at a post-attachment step in the epithelial cells and in the attachment step in the NHDF cells (Fig. 6). It is possible that a receptor involved in attachment of virus in one cell type plays a post-attachment role in the other cell type. Additionally, it is possible that the domains responsible for attachment and fusion within the core glycoprotein complexes are overlapping, but not identical between cell types. This could allow for an entry inhibitor in both cases although not necessarily via the same mechanism. To better understand this observation, this class of inhibitors remains to be further characterized.

Many compounds showed toxicity, as detected by reduced cell number. However, the cells were in medium without serum for 24 h and virus infection can sensitize the cells for cytotoxic effects. The NHDF cells appeared to be more sensitive to the cytotoxic effect than the ARPE-19 cells.

Most of the validated hits belonged to natural products, lead compounds or known drugs, whereas no validated hits were identified among the peptidomimetics (Table 2). Since inhibitors that belong to the peptidomimetics class of compounds can typically effectively block protein-protein interactions, it would have been possible to identify selective inhibitors of virus entry from this class of compounds. A large proportion of the compounds similar to ion channel, GPCR, and kinase inhibitors, as well as optimized lead compounds were found to be cytotoxic. The compounds that inhibited virus entry in a post-attachment phase belonged mainly to kinase and GPCR inhibitor classes. This is particularly interesting because while tyrosine kinase receptors (TKR's) have been proposed as entry receptors, no specific GPCRs have yet been identified as putative receptor for HCMV. Furthermore, selective and specific inhibitors of the proposed HCMV entry-mediating TKR's epidermal growth factor receptor (EGFR) (Wang et al., 2003), and platelet-derived growth factor (Soroceanu et al., 2008), did not inhibit virus entry (data not shown).

Thus, using fluorescent reporter viruses and high-content screening we were able to identify inhibitors of virus entry and to identify the step at which the inhibitors act. Future work will focus on generating resistant virus to these selective inhibitors to identify their targets. The 'known drugs' category of inhibitors consists of specific molecules that target cellular proteins. Further validation of these hits may ultimately lead to the identification of essential cellular factors required for virus entry in specific or multiple cell types. This assay and screening strategy has also led to the identification of nontoxic inhibitors of entry into both epithelial and fibroblasts cells. Inhibitors with this favorable profile can be further optimized to generate anti-viral candidates that can potentially be entered into development.

Acknowledgements

We would like to thank Paul Selzer for fruitful discussions.

References

Bland, J.M., Altman, D.G., 1999. Measuring agreement in method comparison studies. Stat. Methods Med. Res. 8, 135–160.
Bloom, J.D., DiGrandi, M.J., Dushin, R.G., Curran, K.J., Ross, A.A., Norton, E.B., Terefenko, E., Jones, T.R., Feld, B., Lang, S.A., 2003. Thiourea inhibitors of herpes viruses. Part 1: bis-(aryl)thiourea inhibitors of CMV. Bioorg. Med. Chem. Lett. 13, 2929–2932.
Boyle, K.A., Compton, T., 1998. Receptor-binding properties of a soluble form of human cytomegalovirus glycoprotein B. J. Virol. 72 (3), 1826–1833.
Cinque, P., Marenzi, R., Ceresa, D., 1997. Cytomegalovirus infections of the nervous system. Intervirology 40 (2–3), 85–97.
Compton, T., 1995. Towards a definition of the HCMV entry pathway. Scand. J. Infect. Dis. Suppl. 99, 30–32.
Compton, T., Nepomuceno, R.R., Nowlin, D.M., 1992. Human cytomegalovirus penetrates host cells by pH-independent fusion at the cell surface. Virology 191, 387–395.
Compton, T., Nowlin, D.M., Cooper, N.R., 1993. Initiation of human cytomegalovirus infection requires initial interaction with cell surface heparan sulfate. Virology 193 (2), 834–841.
Crisman, T.J., Jenkins, J.L., Parker, C.N., Hill, W.A., Bender, A., Deng, Z., Nettles, J.H., Davies, J.W., Glick, M., 2007. "Plate cherry picking": a novel semi-sequential screening paradigm for cheaper, faster, information-rich compound selection. J. Biomol. Screen. 12, 320–327.
Dankner, W.M., McCutchan, J.A., Richman, D.D., Hirata, K., Spector, S.A., 1990. Localization of human cytomegalovirus in peripheral blood leukocytes by in situ hybridization. J. Infect. Dis. 161 (1), 31–36.
Feire, A.L., Koss, H., Compton, T., 2004. Cellular integrins function as entry receptors for human cytomegalovirus via a highly conserved disintegrin-like domain. Proc. Natl. Acad. Sci. U.S.A. 101 (43), 15470–15475.
Feire, A.L., Roy, R.M., Manley, K., Compton, T., 2010. The glycoprotein B disintegrin-like domain binds beta 1 integrin to mediate cytomegalovirus entry. J. Virol. 84 (19), 10026–10037.
Gerna, G., Percivalle, E., Lilleri, D., Lozza, L., Fornara, C., Hahn, G., Baldanti, F., Revello, M.G., 2005. Dendritic-cell infection by human cytomegalovirus is restricted to strains carrying functional UL131-128 genes and mediates efficient viral antigen presentation to CD8+ T cells. J. Gen. Virol. 86 (Pt 2), 275–284.
Griffiths, P.D., Clark, D.A., Emery, V.C., 2000. Betaherpesviruses in transplant recipients. J. Antimicrob. Chemother. 45 (Suppl. T3), 29–34.
Hahn, G., Revello, M.G., Patrone, M., Percivalle, E., Campanini, G., Sarasini, A., Wagner, M., Gallina, A., Milanesi, G., Koszinowski, U., Baldanti, F., Gerna, G., 2004. Human cytomegalovirus UL131-128 genes are indispensable for virus growth in endothelial cells and virus transfer to leukocytes. J. Virol. 78 (18), 10023–10033.
Ibanez, C.E., Schrier, R., Ghazal, P., Wiley, C., Nelson, J.A., 1991. Human cytomegalovirus productively infects primary differentiated macrophages. J. Virol. 65 (12), 6581–6588.
Jacobson, M.A., 1998. AIDS-related cytomegalovirus retinitis. Drugs Today (Barc.) 34 (5), 409–413.
Jahn, G., Kouzarides, T., Mach, M., Scholl, B.C., Plachter, B., Traupe, B., Preddie, E., Satchwell, S.C., Fleckenstein, B., Barrell, B.G., 1987a. Map position and nucleotide sequence of the gene for the large structural phosphoprotein of human cytomegalovirus. J. Virol. 61 (5), 1358–1367.
Jahn, G., Scholl, B.C., Traupe, B., Fleckenstein, B., 1987b. The two major structural phosphoproteins (pp65 and pp150) of human cytomegalovirus and their antigenic properties. J. Gen. Virol. 68 (Pt 5), 1327–1337.
Jones, T.R., Lee, S.W., Johann, S.V., Razinkov, V., Visalli, R.J., Feld, B., Bloom, J.D., O'Connell, J., 2004. Specific inhibition of human cytomegalovirus glycoprotein B-mediated fusion by a novel thiourea small molecule. J. Virol. 78, 1289–1300.
Kari, B., Gehrz, R., 1992. A human cytomegalovirus glycoprotein complex designated gC-II is a major heparin-binding component of the envelope. J. Virol. 66 (3), 1761–1764.
Ljungman, P., 1996. Cytomegalovirus infections in transplant patients. Scand. J. Infect. Dis. Suppl. 100, 59–63.
Menard, C., Wagner, M., Ruzsics, Z., Holak, K., Brune, W., Campbell, A.E., Koszinowski, U.H., 2003. Role of murine cytomegalovirus US22 gene family members in replication in macrophages. J. Virol. 77 (10), 5557–5570.
Nowlin, D.M., Cooper, N.R., Compton, T., 1991. Expression of a human cytomegalovirus receptor correlates with infectibility of cells. J. Virol. 65 (6), 3114–3121.
Roby, C., Gibson, W., 1986. Characterization of phosphoproteins and protein kinase activity of virions, noninfectious enveloped particles, and dense bodies of human cytomegalovirus. J. Virol. 59 (3), 714–727.

Ruger, B., Klages, S., Walla, B., Albrecht, J., Fleckenstein, B., Tomlinson, P., Barrell, B., 1987. Primary structure and transcription of the genes coding for the two virion phosphoproteins pp65 and pp71 of human cytomegalovirus. J. Virol. 61 (2), 446–453.

Ryckman, B.J., Rainish, B.L., Chase, M.C., Borton, J.A., Nelson, J.A., Jarvis, M.A., Johnson, D.C., 2008. Characterization of the human cytomegalovirus gH/gL/UL128-131 complex that mediates entry into epithelial and endothelial cells. J. Virol. 82 (1), 60–70.

Schmolke, S., Drescher, P., Jahn, G., Plachter, B., 1995. Nuclear targeting of the tegument protein pp65 (UL83) of human cytomegalovirus: an unusual bipartite nuclear localization signal functions with other portions of the protein to mediate its efficient nuclear transport. J. Virol. 69 (2), 1071–1078.

Shukla, D., Liu, J., Blaiklock, P., Shworak, N.W., Bai, X., Esko, J.D., Cohen, G.H., Eisenberg, R.J., Rosenberg, R.D., Spear, P.G., 1999. A novel role for 3-O-sulfated heparin sulfate in herpes simplex virus 1 entry. Cell 99, 13–22.

Sinzger, C., 2008. Entry route of HCMV into endothelial cells. J. Clin. Virol. 41 (3), 174–179.

Sinzger, C., Jahn, G., 1996. Human cytomegalovirus cell tropism and pathogenesis. Intervirology 39 (5–6), 302–319.

Sinzger, C., Kahl, M., Laib, K., Klingel, K., Rieger, P., Plachter, B., Jahn, G., 2000. Tropism of human cytomegalovirus for endothelial cells is determined by a post-entry step dependent on efficient translocation to the nucleus. J. Gen. Virol. 81 (Pt 12), 3021–3035.

Somogyi, T., Michelson, S., Masse, M.J., 1990. Genomic location of a human cytomegalovirus protein with protein kinase activity (PK68). Virology 174 (1), 276–285.

Soroceanu, L., Akhavan, A., Cobbs, C.S., 2008. Platelet-derived growth factor-alpha receptor activation is required for human cytomegalovirus infection. Nature 455 (7211), 391–395.

Spear, P.G., Longnecker, R., 2003. Herpesvirus entry: an update. J. Virol. 77 (19), 10179–10185.

Sweet, C., 1999. The pathogenicity of cytomegalovirus. FEMS Microbiol. Rev. 23 (4), 457–482.

van Den Pol, A.N., Mocarski, E., Saederup, N., Vieira, J., Meier, T.J., 1999. Cytomegalovirus cell tropism, replication, and gene transfer in brain. J. Neurosci. 19 (24), 10948–10965.

Varnum, S.M., Streblow, D.N., Monroe, M.E., Smith, P., Auberry, K.J., Pasa-Tolic, L., Wang, D., Camp 2nd, D.G., Rodland, K., Wiley, S., Britt, W., Shenk, T., Smith, R.D., Nelson, J.A., 2004. Identification of proteins in human cytomegalovirus (HCMV) particles: the HCMV proteome. J. Virol. 78 (20), 10960–10966.

Wang, D., Shenk, T., 2005a. Human cytomegalovirus UL131 open reading frame is required for epithelial cell tropism. J. Virol. 79 (16), 10330–10338.

Wang, D., Shenk, T., 2005b. Human cytomegalovirus virion protein complex required for epithelial and endothelial cell tropism. Proc. Natl. Acad. Sci. U.S.A. 102 (50), 18153–18158.

Wang, X., Huang, D.Y., Huong, S.M., Huang, E.S., 2005. Integrin alphavbeta3 is a coreceptor for human cytomegalovirus. Nat. Med. 11 (5), 515–521.

Wang, X., Huong, S.M., Chiu, M.L., Raab-Traub, N., Huang, E.S., 2003. Epidermal growth factor receptor is a cellular receptor for human cytomegalovirus. Nature 424 (6947), 456–461.

Warming, S., Costantino, N., Court, D.L., Jenkins, N.A., Copeland, N.G., 2005. Simple and highly efficient BAC recombineering using galK selection. Nucleic Acids Res. 33 (4), e36.

Whitley, R.J., 2004. Congenital cytomegalovirus infection: epidemiology and treatment. Adv. Exp. Med. Biol. 549, 155–160.

Yu, D., Smith, G.A., Enquist, L.W., Shenk, T., 2002. Construction of a self-excisable bacterial artificial chromosome containing the human cytomegalovirus genome and mutagenesis of the diploid TRL/IRL13 gene. J. Virol. 76 (5), 2316–2328.

Zhang, J.H., Chung, T.D.Y., Oldenburg, K.R., 1999. A simple statistical parameter for use in evaluation and validation of high throughput screening assays. J. Biomol. Screen. 4, 67–73.